JOURNAL OF CATALYSIS 85, 260–266 (1984)

Catalysts for Low-Temperature Methanol Synthesis. Preparation of Cu–Zn–Al Mixed Oxides via Hydrotalcite-like Precursors

Cu–Zn–Al-mixed oxides are well-known as catalysts for methanol synthesis and the gas shift reaction at low temperature (*1–5*) and references in (*4*)). In a previous paper we have investigated the influence of the preparation conditions on the nature of the precursors (*6*). By precipitation at constant pH, we obtained a compound with a structure similar to that of the natural hydrotalcite, $Mg_6Al_2(OH)_{16}CO_3 \cdot 4H_2O$. Whether the compound was obtained pure or not depended on the ratio between the elements (*7*).

The aim of this paper was to carry out an in-depth investigation into the nature and characteristics of this ternary compound and its evolution with the calcination temperature until the formation of the oxide phases.

EXPERIMENTAL

The compounds have been prepared by precipitation at constant pH with $NaHCO_3$ (*7*); to obtain an acceptable hydrotalcite-like phase yield, the Cu–Al system was prepared by decomposing in vacuum the copper ammoniacal complex on γ-Al_2O_3 (Akzo-Chemie, grade E) (*6, 8*).

XRD powder patterns were collected using a Philips goniometer, equipped with a stepping motor and automated by means of a General Automation 16/240 computer. The radiation used was the nickel-filtered Cu$K\bar{\alpha}$ (λ = 0.15418 nm) and, for an accurate determination of d values, silicon was employed as an internal standard. Observed d spacings were indexed on the basis of a trigonal unit cell, and the space group $R\bar{3}m$, in a similar way to the data reported for the natural hydrotalcite (*9*). The cell constants were refined using a least-squares program.

For the calcined samples, both the phase composition and the crystal sizes were determined by a profile-fitting method, comparing the observed profiles with the computed ones, calculated, according to Allegra *et al.* (*10*), from structural data (*11–13*).

The ESR spectra were recorded on a Varian E-112 X-band spectrometer, equipped with a variable temperature accessory, using a DPPH sample as a reference standard. The spectra were doubly integrated by means of a Varian E 900 ESR Data Acquisition System. Relative spin density was obtained through a Varian standard weak pitch on KCl.

RESULTS AND DISCUSSION

In addition to the element ratio, also the preparation steps influence the formation of the different phases: we observed the presence of a hydrotalcite-like compound already after the precipitation. By washing the precipitates to eliminate the nitrate ions and to reduce the sodium content to less than 0.03% (as Na_2O), we destroyed partially the hydrotalcite-like phase, forming for example the more stable malachite. This phenomenon considerably increased by heating the precipitate as a slurry to make easier the elimination of the sodium ions with a brief washing.

In all cases, however, the hydrotalcite-like phase was already present in the first precipitate and no aging procedure was necessary for its formation. A typical X-ray powder pattern of a pure hydrotalcite-like phase dried at 90°C is shown in Fig. 2 (pat-

0021-9517/84 $3.00

TABLE 1

X-Ray Powder Data of the $(Cu_xZn_{6-x})Al_2(OH)_{16}CO_3 \cdot 4H_2O$ Series

h k l	x = 0		I/I₀	x = 2		I/I₀	x = 3		I/I₀	x = 6		I/I₀
	d_{obs}	d_{calc}		d_{obs}	d_{calc}		d_{obs}	d_{calc}		d_{obs}	d_{calc}	
0 0 3	7.596	7.600	100	7.525	7.540	100	7.506	7.485	100	7.613	7.610	100
0 0 6	3.800	3.800	44	3.770	3.770	43	3.749	3.743	42	3.807	3.805	40
1 0 1	2.644	2.645	9	2.640	2.642	8	2.642	2.641	8	—	2.637	—
0 1 2	2.593	2.593	42	2.589	2.589	41	2.581	2.588	42	2.586	2.586	40
1 0 4	2.412	2.413	11	2.404	2.407	9	2.404	2.404	10	—	2.408	—
0 1 5	2.299	2.300	33	2.293	2.293	35	2.287	2.289	33	2.296	2.295	30
1 0 7	2.062	2.062	5	2.053	2.054	5	2.049	2.048	5	—	2.059	—
0 1 8	1.946	1.946	30	1.936	1.937	29	1.928	1.931	28	1.944	1.944	30
1 0 10	1.732	1.732	11	1.723	1.723	10	1.717	1.716	11	1.731	1.731	10
0 1 11	1.636	1.636	5	1.626	1.627	5	1.618	1.619	5	—	1.636	—
1 1 0	1.538	1.538	13	1.535	1.536	12	1.536	1.536	11	1.533	1.533	10
1 1 3	1.507	1.507	15	1.505	1.505	15	1.505	1.504	14	1.503	1.502	10
1 0 13	1.464	1.465	5	1.457	1.456	4	1.450	1.449	5	—	1.465	—
1 1 6	1.425	1.425	7	1.423	1.422	6	1.420	1.421	6	—	1.422	—

Note. d_{hkl} spacings (nm) × 10; I/I_0 from integrated areas.

tern *a*), while Table 1 reports the X-ray powder data for the different Cu/Zn ratios.

All characteristics of X-ray data and spectra suggest an isostructurality with the minerals hydrotalcite, pyroaurite, and stichtite, the crystal structures of which have been reported by Allmann (*14, 15*). Therefore, the structure of our compounds can be described as an alternation of positively charged brucite-like layers $[M_6^{II}M_2^{III}(OH)_{16}]^{2+}$, in which all cations are randomly distributed among the octahedral position, and disordered negatively charged interlayers $[CO_3 \cdot 4H_2O]^{2-}$. The OH layer sequence is the rhombohedral -BC-CA-AB-BC- (A, B, C, or three threefold axes in $x, y = 0, 0; \frac{2}{3}, \frac{1}{3}; \frac{1}{3}, \frac{2}{3}$).

On the basis of the hydrotalcite structure, the changes in the lattice parameter *a* should be directly related to the changes in the thickness of the brucite-like cationic layer, the variations are small, due to the similar ionic radii of Cu^{2+} and Zn^{2+} hexacoordinates (*16*). The length of the *c* axis mainly depends on the nature and steric requirements of the anions and the content of water molecules in the interlayer.

The best packing conditions are obtained when the atomic ratio r = Cu/ Cu + Zn is close to 0.5, to which correspond also the best conditions for the ternary phase formation and the greatest phase purity.

We may note from Fig. 1 that in the range of r from 0 to 0.5, in which the hydrotalcite-like phase is always pure, both *a* and *c* decrease with the rise of r, the variation of *c* being larger than that of *a*. In the range of r from 0.5 to approximately 0.9, in which the ternary hydrotalcite phase can no longer be obtained pure, being always accompanied by a malachite phase, which increases with the copper content in the sample, the cell parameters vary slightly and randomly within a range of values close to those for $r = 0.5$. When r is greater than about 0.9, only a malachite phase can be obtained with the preparation of Ref. (*7*); a Cu/Al binary hydrotalcite-like phase has nevertheless been prepared, mixed with large amounts of CuO and alumina, operating in another way (*6, 8*). On the other hand, a pure hydrotalcite-like phase was recently obtained also with $r = 0.5$ and Al 31%: this is consistent with the findings of Allmann and other authors (*15, 17, 18*), which identify phases with the same structure in the range Me^{3+}/

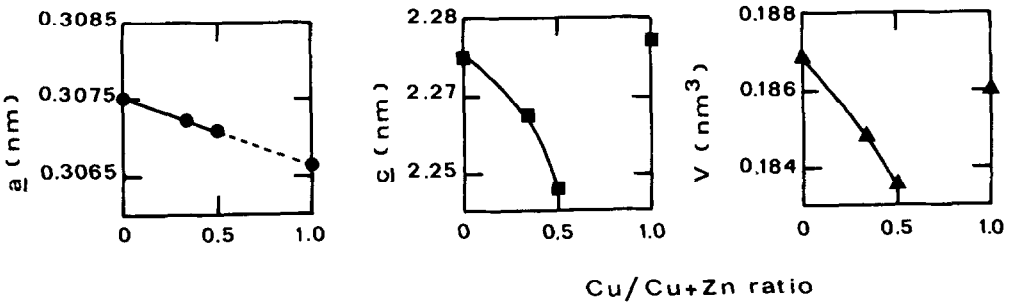

FIG. 1. Plots of crystal parameters against the atomic ratio Cu/ Cu + Zn for the (Cu_xZn_{6-x}) $Al_2(OH)_{16}CO_3 \cdot 4H_2O$ series.

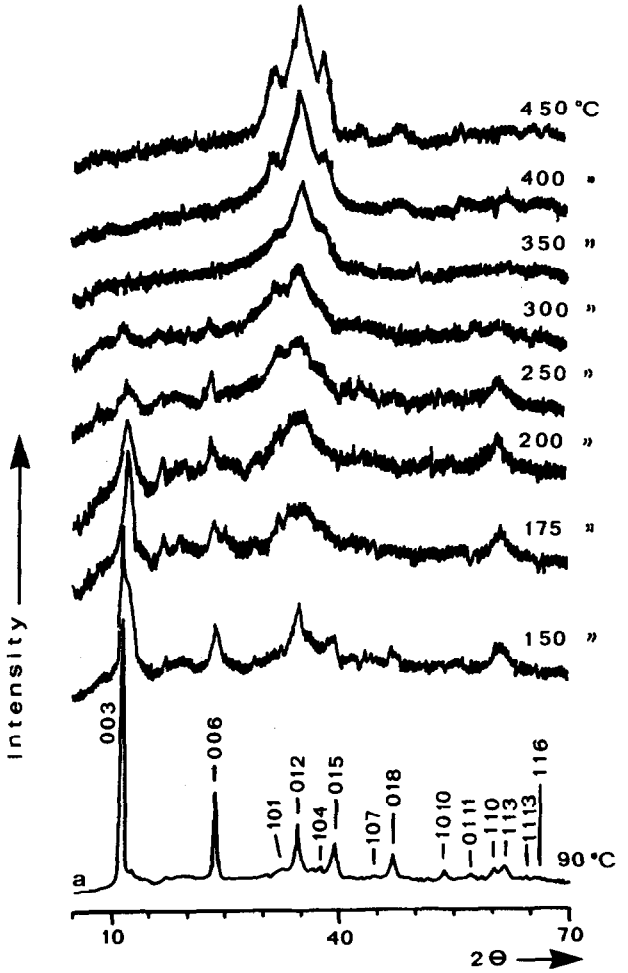

FIG. 2. X-Ray powder patterns of the pure hydrotalcite-like phase calcined at different temperatures in the range 90–450°C (every step took 4 h).

$Me^{2+} + Me^{3+} = 0.20$ to 0.33. All the parameters were the same as for the sample with the same atomic ratio, and 24% aluminum content.

In Fig. 2 we have reported the X-ray patterns of the pure hydrotalcite-like phase calcined at different temperatures. The disappearance of the hydrotalcite-like phase pattern may already be observed at 150°C, with the appearance of a pattern with relatively broad lines, very similar to hydrozincite and/or aurichalcite ones. In the range 150–350°C, the progressive decrease of the hydroxycarbonate phases and the consequent increase in the oxide phases may be observed. At 350°C the total conversion into oxides is reached, with minimum crystal size. At higher temperature, up to 450°C, only a small amount of sintering phenomena is observed.

The ESR spectra of the hydrotalcite-like phase calcined in the range 90–450°C are reported in Fig. 3: at the first calcination steps, a very large band, several thousand Gauss wide, probably caused by the Cu^{2+} ions in the hydrotalcite crystal lattice, may be observed. As the calcination temperature increases, the intensity of this signal

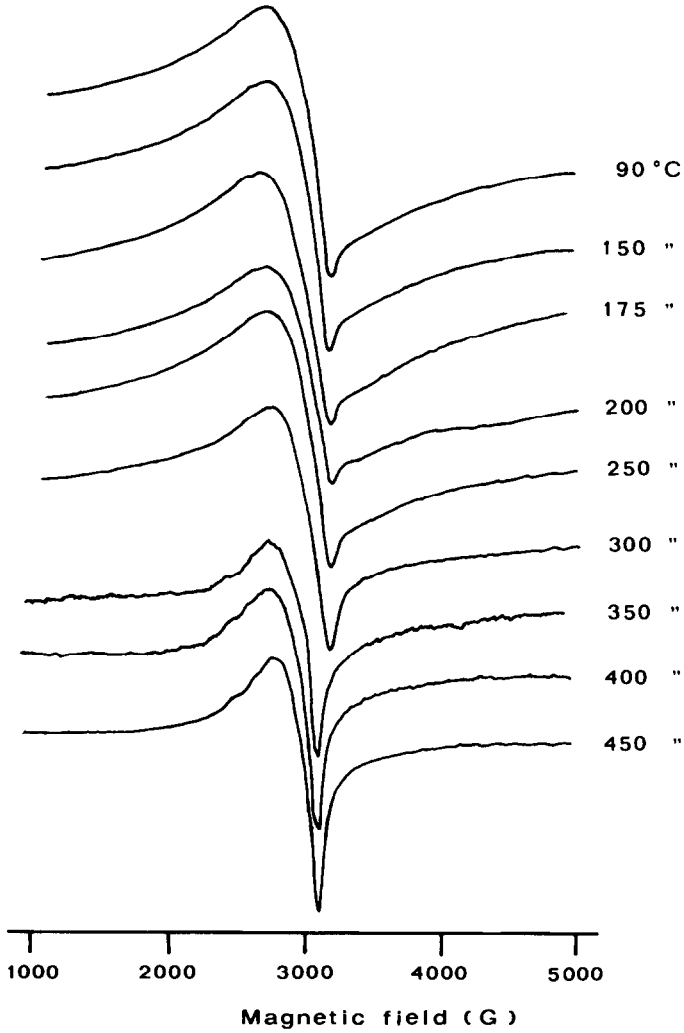

FIG. 3. ESR spectra of the pure hydrotalcite-like phase calcined at different temperatures in the range 90–450°C (every step took 4 h).

tends to disappear. The main feature of the ESR spectrum of the sample calcined at 350°C is the presence of two overlapping signals, an anisotropic line shape with a hyperfine structure ($g_{\parallel} = 2.31$, $A_{\parallel} = 15$ mT, $g_{\perp} = 2.07$, and $A_{\perp}$ unresolved), and a broad symmetric line at $g \cong 2.15$ with $\Delta H \cong 500$ G.

In the past, Schischkov *et al.*, in a study of similar systems, had attributed the anisotropic signal to Cu^{2+} ions stabilized in the octahedral vacancies of the crystal lattice of $ZnAl_2O_4$, whereas they attributed the symmetric signal to Cu^{2+} ions in the crystal lattice of the spinel $CuAl_2O_4$ (*19, 20, 21*).

However, a large fraction of the copper appears to escape detection by ESR, probably on account of the spin pairing. The percentage of the measured ESR intensity with respect to the theoretical total intensity due to Cu^{II} is correlated with the dispersion of the copper in the diamagnetic phases.

Attributing this effect to spinel phases only, according to Refs. (19–21), there should be a linear relation between the intensity of the ESR signal and the Cu/Al ratio. This relation is however poorly supported (correlation index 0.73), and it is doubtless better to consider the Cu/ Zn + Al ratio (correlation index 0.93) (Figs. 4A and B, respectively). Both ZnO and the spinels (MAl_2O_4) therefore, in the systems analyzed, contribute to the magnetic dilution of the copper.

After calcination at 350°C for 24 h, the total decomposition of the precursors, with the formation of CuO and ZnO was revealed by means of X-ray diffraction. While on the one hand there has been no evidence of the presence of free Al_2O_3, probably owing to the very small quantity of it and/or to its amorphous state, some evidence, albeit slight, of the presence of type MAl_2O_4 (M = Cu,Zn) spinels has been obtained.

From Table 2, one may note how mixed systems supply for both the oxides, much smaller crystallites than those of the CuO and ZnO samples obtained from malachite and hydrozincite, respectively. Furthermore, it has been observed that the lowest

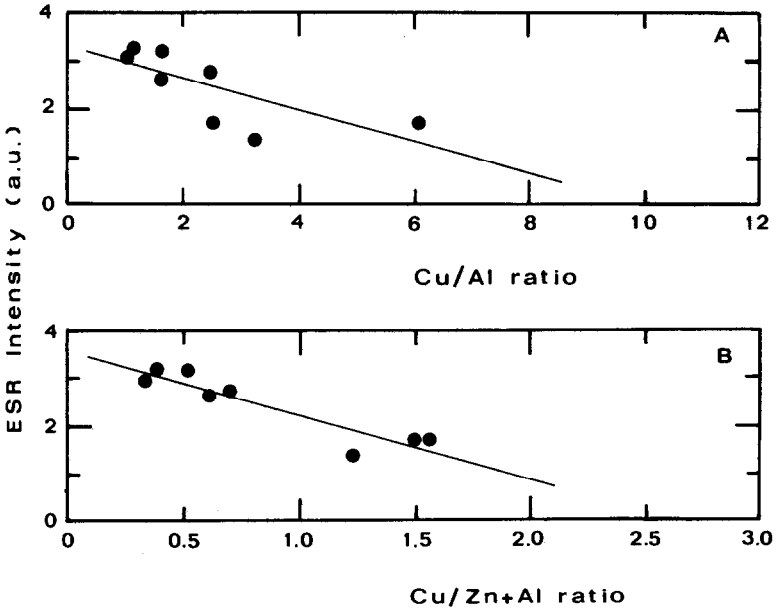

FIG. 4. Intensity of the ESR signal as a function of the Cu/Al ratio (A) and of the Cu/Zn + Al ratio (B) in the samples calcined at 350°C for 24 h.

TABLE 2

Crystal Size (nm) of CuO and ZnO Obtained by Calcination of the Precursors at 350°C for 24 h

Identified compounds (after drying at 90°C)	Ratio		Crystal size (nm) (after calcination at 350°C for 24 h)	
	Cu/Zn	Cu + Zn/Al	CuO	ZnO
HY; M	2.0	9.0	6.0	6.0
HY; M	2.0	4.9	6.0	4.0
HY; M	2.0	3.2	6.0	2.5
M; HY	1.0	9.0	6.0	7.0
HY; M	1.0	4.9	3.6	4.4
HY	1.0	3.2	3.0	4.6
HY; quasi-amorphous phases[a]	0.5	9.0	3.6	7.0
HY; quasi-amorphous phases[a]	0.5	4.9	3.0	5.0
HY	0.5	3.2	4.0	6.0
HY	1.0	2.2	<1.5	<1.5
Malachite[b]	—	—	9.5	—
Hydrozincite[b]	—	—	—	17.0

[a] X-Ray patterns similar to those of hydrozincite and/or aurichalcite. HY = hydrotalcite; M = malachite.

[b] From E. Merck, Germany.

values were obtained in the case of samples in which the hydrotalcite-like phase was prevalent and for the element of which less was present.

It does not seem necessary for this ternary phase to be pure, its considerable prevalence over any satellite phase being sufficient. However, the lowest crystal sizes were obtained for the sample with the highest aluminum content.

REFERENCES

1. Natta, G., *in* "Catalysis" (P. H. Emmet, Ed.), Vol. III, Chap. 8, Reinhold, New York, 1953.
2. Davies, P., and Hall, A. J., U.S. Pat. 3,391,037 (1976).
3. Ruggeri, O., Trifirò, F., and Vaccari, A., *J. Solid State Chem.* **42,** 120 (1982).
4. Klier, K., *in* "Advances in Catalysis" (D. D. Eley, H. Pines, and P. B. Weisz, Eds.), Vol. 31, p. 243. Academic Press, New York, 1982.
5. Courty, P., and Marcilly, C., *in* "Preparation of Catalysts III" (G. Poncelet, P. Grange, and P. A. Jacobs, Eds.), p. 485. Elsevier, Amsterdam, 1983.
6. Ruggeri, O., Tredici, A., Trifirò, F., and Vaccari, A., 8° Simposio Iberoamericano de Catalisis, Huelva, Spain, July 12–17, 1982.
7. Gherardi, P., Ruggeri, O., Trifirò, F., Vaccari, A., Del Piero, G., Manara, G., and Notari, B., *in* "Preparation of Catalysts III" (G. Poncelet, P. Grange, and P. A. Jacobs, Eds.), p. 723. Elsevier, Amsterdam, 1983.
8. Echevin, B., Ph.D. thesis, Univ. C. Bernard, Lyon, France, 1972.
9. Roy, D. M., Roy, R., and Osborn, E. F., *Amer. J. Sci.* **251,** 337 (1953).
10. Allegra, G., and Ronca, G., *Acta Crystallogr. A* **34,** 1006 (1978).
11. Asbrink, S., and Narrby, L. J., *Acta Crystallogr. B* **26,** 8 (1970).
12. Abrabams, G. C., and Bernstein, J. L., *Acta Crystallogr. B* **25,** 1233 (1969).
13. Ghose, S., *Acta Crystallogr.* **17,** 1051 (1964).
14. Allmann, R., *Acta Crystallogr. B* **24,** 972 (1968).
15. Allmann, R., and Jepsen, H. P., *N. Jb. Miner. Monatsh.* 544 (1969).
16. Shannon, R. D., and Prewitt, C. T., *Acta Crystallogr. B* **25,** 925 (1969).
17. Brindley, G. W., and Kikkawa, S., *Amer. Mineral.* **64,** 836 (1979).
18. Miyata, S., *Clays Clay Mineral.* **28,** 50 (1980).
19. Andreev, A. A., and Schischkov, D. S., *Z. Chem.* **15,** 200 (1975).

20. Andreev, A. A., Schopov, D. M., Schischkov, D. S., and Kassabova, N. A., *Z. Chem.* **16,** 457 (1976).
21. Schischkov, D. S., Kassabova, N. A., Andreev, A. A., and Schopov, D. M., *in* "Proceedings, 4th International Symposium on Heterogeneous Catalysis" (D. M. Schopov, A. A. Andreev, A. Palazov, and L. Petrov, Eds.), Vol. 1, p. 169. Publ. House of the Bulgarian Academy of Sciences, Sofia, 1979.

C. BUSETTO
G. DEL PIERO
G. MANARA

Assoreni Co., Via Fabiani
20097 San Donato Milanese
Milan, Italy

F. TRIFIRÒ[1]
A. VACCARI

Facoltà di Chimica Industriale
Viale del Risorgimento 4
40136 Bologna, Italy

Received March 1, 1983

[1] To whom correspondence should be addressed.